Pulmonary, gastrointestinal and urogenital pharmacology

# Development of an experimental rat model of hyperammonemic encephalopathy and evaluation of the effects of rifaximin

CrossMark

Satoru Tamaoki [a,*], Hiroyuki Suzuki [a], Mami Okada [a], Norio Fukui [b], Mitsui Isobe [b], Tomoyuki Saito [a]

[a] Pharmacological Research Department, ASKA Pharmaceutical Co., Ltd., 5-36-1, Shimosakunobe, Takatsu-ku, Kawasaki 213-8522, Japan
[b] Safety Research Department, ASKA Pharmaceutical Co., Ltd., 5-36-1, Shimosakunobe, Takatsu-ku, Kawasaki 213-8522, Japan

## ARTICLE INFO

## ABSTRACT

Hepatic encephalopathy (HE) is a neuropsychiatric syndrome associated with hepatic dysfunction. However, the precise mechanism of HE is unclear. To elucidate the mechanism, we developed a new rat model of HE with coma using a combination of subcutaneous splenic transposition, partial hepatectomy and portal vein stenosis. In this model, blood ammonia levels increase in the postcaval vein over time and markedly increase in the cerebrospinal fluid (CSF). The distribution of ammonia in the various blood vessels in the HE model suggests that the origin of peripheral blood and CSF ammonia is the mesenteric veins that drain blood from the gastrointestinal tract. Behavioral analysis revealed decreased pain response, increased passivity, and decreased pinna and corneal reflexes, followed by the development of coma. The development of coma in this model was frequent and reproducible. Increased S100 calcium-binding protein B (S100B: a biomarker for brain injury) in venous blood, as well as damaged brain tissue, increased intracranial pressure and cerebral edema were observed in rats with coma. A very high correlation was observed between the blood ammonia concentration in the postcaval vein and the onset of coma. Rifaximin, a poorly absorbed antibiotic that targets gut flora, significantly improved symptoms of HE. Based on these results, our rat model appears to reflect the pathological state of HE associated with acute liver failure and may be a useful model for analysis of hyperammonemic encephalopathy.

## 1. Introduction

Hepatic encephalopathy (HE) is an important complication of chronic and acute liver disease (Riordan and Williams, 1997; Sturgeon and Shawcross, 2014). Previously, HE has been classified into three types: Type A, HE associated with acute liver failure (ALF); type B, HE associated with portal-systemic shunting without hepatocellular disease; and type C, HE associated with underlying cirrhosis and portal hypertension or portal-systemic shunts (Ferenci et al., 2002). The pathophysiology of HE is not completely understood, although there is agreement on the important role of neurotoxins, particularly ammonia (Romero-Gómez et al., 2015). Ammonia is produced from several organs, such as kidneys and muscle, and its concentration is highest in the portal venous system in dog, sheep and horse (Hahn et al., 1893; Nencki and Zaleski, 1895; Nencki et al., 1896). In humans, portal ammonia

is presumed to be derived from both the urease activity of the colonic bacteria and the deamination of glutamine in the small intestine (Romero-Gómez et al., 2015). Therefore, we examined the distribution of blood ammonia in rats, given its fundamental role in the pathology of HE.

In clinical practice, the blood ammonia level is widely used for diagnosing HE; blood levels correlate with an increased risk of encephalopathy (Bernal et al., 2007). However, the correlation between blood ammonia levels and HE severity is not consistent (Bosoi et al., 2011; Ong et al., 2003; Shawcross et al., 2011). In the absence of an appropriate animal model of HE, there may be discrepancies between experimental results and clinical signs. For example, a drug-induced hepatotoxicity model has been shown to induce definite pathological lesions, but does not reproduce the same behavioral signs observed in HE patients (Butterworth et al., 2009). Coma is an important behavioral change in HE patients and should be evaluated as a pathognomonic feature (Leise et al., 2014; Vilstrup et al., 2014). Other models, for example the portal-systemic anastomosis model, require a high degree of microsurgical skill and lack general versatility (Funovics et al., 1975; Jover et al., 2005). We thus established a new rat model of HE using an efficient surgical method that resulted in hyperammonemia and

---

* Corresponding author.
E-mail addresses: tamaoki-s@aska-pharma.co.jp (S. Tamaoki), suzuki-h3@aska-pharma.co.jp (H. Suzuki), okada-m@aska-pharma.co.jp (M. Okada), fukui-n@aska-pharma.co.jp (N. Fukui), isobe-m@aska-pharma.co.jp (M. Isobe), saito-t1@aska-pharma.co.jp (T. Saito).

coma. The objectives of this study were to develop a reliable HE model and clarify the correlation between blood ammonia levels and the onset of coma. Rifaximin is an oral, nonsystemic, broad-spectrum antibiotic that targets gut flora (Bass et al., 2010) and is used clinically to reduce serum ammonia derived from the gastrointestinal (GI) tract. We thus used rifaximin to investigate the role of ammonia in our HE model.

## 2. Materials and methods

### 2.1. Animals

All study procedures were carried out after approval of the protocol by the Animal Research Committee of ASKA Pharmaceutical Co., Ltd. based on the criteria, "Rules for the Care and Use of Laboratory Animals". Male Sprague Dawley rats (Charles River Laboratories Japan, Inc., Yokohama) weighing 170–230 g were used. The animals were maintained at constant temperature (22 °C) on a 12 h light/dark cycling schedule (8:00 on and 20:00 off) with free access to food and water.

### 2.2. Drugs

Dosing formulations were freshly prepared on the day of use and administered orally in doses ranging from 2 to 5 ml/kg. Rifaximin was manufactured by Alfa Wassermann S.p.A., Bologna, Italy. Tween® 80 was obtained from MP Biomedicals, LLC, Santa Ana, CA.

### 2.3. Experimental design and surgical procedure

Following subcutaneous splenic transposition (SST), rats were orally administered either vehicle (0.5% Tween 80) or rifaximin (0.3, 3 and 30 mg/kg) once daily for 3 days. Three hours after the final dose, animals underwent 70% partial hepatectomy and portal vein stenosis to induce encephalopathy. The time of coma onset was monitored out to 24 h after HE-inducing surgery. Coma was defined as loss of the righting reflex. At the onset of coma or at 24 h after surgery, blood was collected from various vessels for determination of ammonia concentration.

### 2.4. Subcutaneous splenic transposition (SST)

SST was performed according to the method described by Di Domenico et al. (2007). Animals were placed in the dorsal position under isoflurane anesthesia (Wako Pure Chemical Industries, Ltd., Osaka, Japan) and an approximately 1 cm incision was made on the skin below the left costal arch. A subcostal pouch was created laterally in the subcutaneous tissue. The spleen was decapsulized and placed into the pouch. Animals were allowed to recover for 4–6 weeks in order to allow for the development of collateral blood vessels around the spleen.

### 2.5. Partial hepatectomy and portal vein stenosis

The animals were placed in a dorsal position under isoflurane anesthesia and the abdomen was incised to remove 3 lobes of the liver (right, left medial and left lateral), which accounted for approximately 70% of the total liver weight (Nikfarjam et al., 2004). The portal vein and a stainless steel tube (outer diameter 0.5 mm) were ligated using a surgical suture. The steel tube was then removed, leaving the vessel ligated to approximately 0.5 mm. In this manner, blood from the portal vein was shunted into the systemic circulation.

### 2.6. Determination of ammonia and S100 calcium-binding protein B (S100B)

The ammonia levels in blood and cerebrospinal fluid (CSF) were assayed according to the enzymatic cycling method (Yamaguchi et al., 2005). A small sample (50-100 µl) was taken from the vessel or cerebral ventricle, mixed with a deproteinizing agent (Kanto Chemical Co., Inc., Tokyo, Japan) and centrifuged. Ammonia levels in the supernatant were measured using the Ammonia Assay Kit (Kanto Chemical Co., Inc., Tokyo, Japan). Serum levels of S100B were assessed by a sandwich enzyme immunoassay (Rat S100B ELISA kit, Uscn Life Science Inc., China).

### 2.7. Behavioral procedures

Behavioral tests were performed by blinded researchers at 1, 6, 12 and 24 h after HE-inducing surgery. Animals were first placed in a transparent box ($345 \times 403 \times 177$ mm$^3$) and observed for signs of abnormal behavior. A battery of Irwin's basic neurological tests (Irwin, 1968; pain response, pinna reflex, corneal reflex, righting reflex and passivity) was then performed. Behavioral tests were scored on a scale of 0–4 (normal score $= 0$, maximal score $= 4$).

### 2.8. Histological analysis

Animals were euthanized by exsanguination under anesthesia at various time points following surgery. The brain was removed and immediately fixed in 10% neutral buffered formalin. The cerebrum including the hippocampus was trimmed. The tissues were embedded in paraffin wax and sliced into 4 µm sections. Sections were stained with hematoxylin and eosin for histopathological examination.

### 2.9. Intracranial pressure (ICP) monitoring

Following HE-inducing surgery, the midline skin was incised to expose the atlanto-occipital membrane. The cisterna magna was stereotaxically punctured with a 25 G needle, which was connected to a pressure transducer via PE50 tubing. The needle was confirmed to be correctly placed in the subarachnoid space when ICP immediately increased after applying abdominal pressure. The punctured site was sealed with a drop of glue to prevent CSF leakage. A syringe column containing artificial CSF (115 mM NaCl, 5 mM KCl, 1.5 mM CaCl$_2$, 1.3 mM MgCl$_2 \cdot$6H$_2$O, 35 mM NaHCO$_3$, 1.25 mM NaH$_2$PO$_4$ and 10 mM glucose; all chemicals from Sigma-Aldrich, St. Louis, MO) was also connected to the transducer. During the procedure, body temperature was monitored using an intraperitoneal thermistor and maintained at 37 °C with a ventral heating pad. Under these conditions, ICP was measured continuously for 12 h.

### 2.10. Quantification of brain water content

At the end of the experiment, animals were euthanized by exsanguination under anesthesia and the brain was extracted. Brain tissues were weighed and placed in an electro-thermostatic baking oven at 105 °C for 48 h until a constant dry weight was obtained or until the difference between 2 consecutive dry weights was less than 0.0001 g. The brain water content of each sample was calculated according to the following formula:

Brain water content = (Wet weight–Dry weight)/Wet weight ×

100%

## 2.11. Statistical analysis

Statistical analysis was performed using SAS Pre-Clinical Package Ver. 5.0 (SAS Institute Japan). Dose-response was determined using analysis of variance (ANOVA) followed by a non-parametric or parametric Dunnett's multiple comparison test. Comparisons between groups were made using Student's *t*-test or the Wilcoxon test.

The coma onset time was monitored out to 24 h after HE-inducing surgery and was analyzed using the Kaplan-Meier method and a log-rank test. All analyses were performed using Prism 5 for Windows (version 5.0, GraphPad Software Inc., San Diego, CA).

## 3. Results

### 3.1. Blood ammonia levels in normal rats

Ammonia concentrations in the blood from the abdominal aorta and the mesenteric, portal and postcaval veins were first determined in normal rats (Fig. 1). The ammonia concentration in the abdominal aorta was 62.8 ± 13.9 μg/dl. In contrast, mesenteric venous blood, which drains from the GI tract, contained about a 20-fold higher concentration of ammonia, 1588.4 ± 408.7 μg/dl. The ammonia concentration in the portal blood was 644.1 ± 143.2 μg/dl. The blood ammonia level was comparable between the abdominal aorta and postcaval vein.

### 3.2. Onset of coma and blood ammonia levels in the HE model

HE was induced in rats by a combination of SST, partial hepatectomy and portal vein stenosis, and blood ammonia concentrations and coma onset were subsequently measured. When either partial hepatectomy or portal vein stenosis was performed on rats with SST, no appreciable changes were noted in blood ammonia concentrations (Fig. 2A). This fact indicates that blood ammonia produced in the GI tract can be effectively metabolized by approximately 30% of the liver and may not be affected by hemodynamic changes. Furthermore, in the animals in which the blood
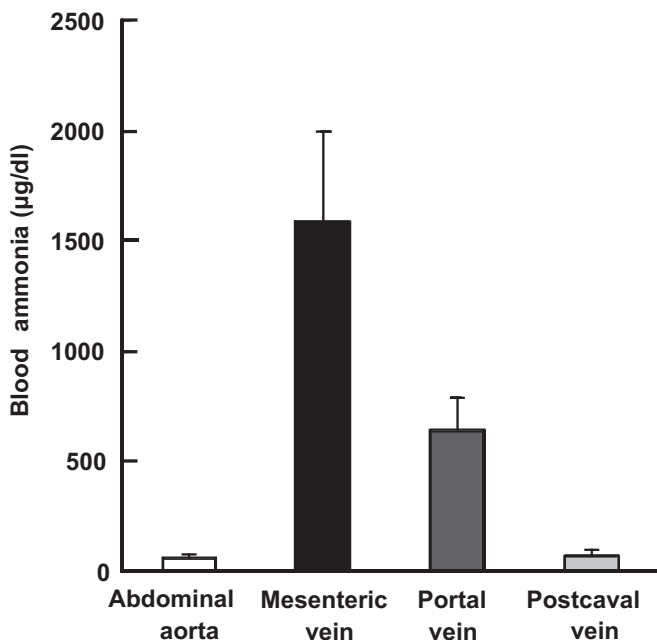


Fig. 1. Blood ammonia levels in various blood vessels in normal rats. Ammonia concentration was measured in blood collected from the abdominal aorta and the mesenteric, portal and postcaval veins. Data represent the mean ± S.D. (*n*=8).
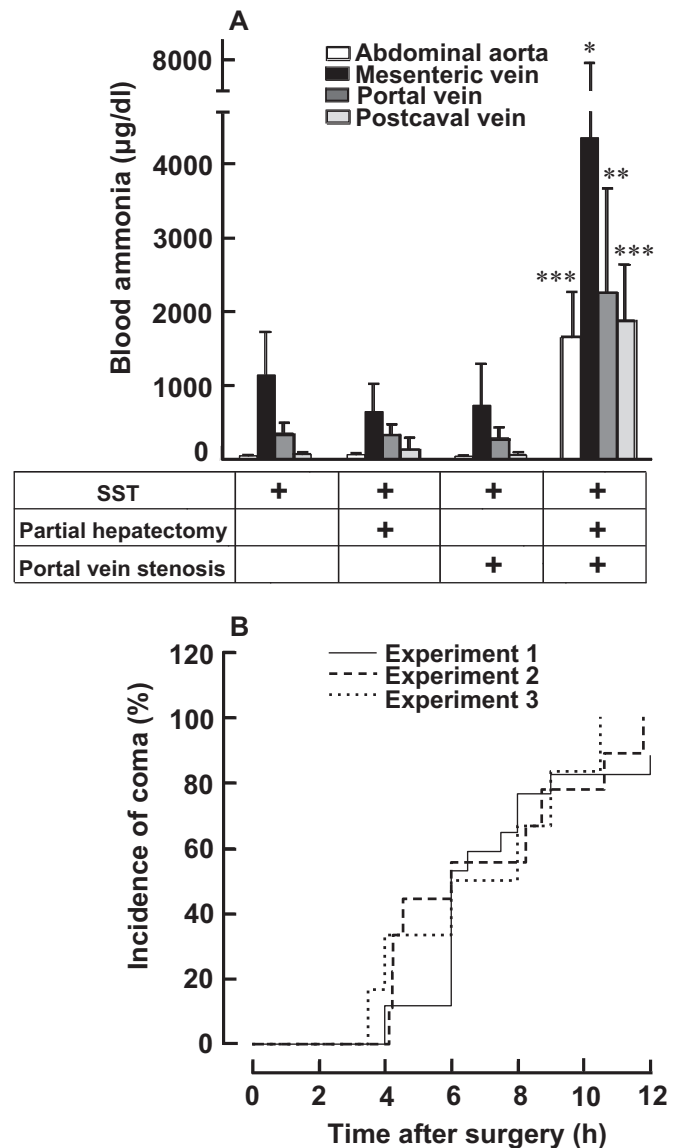


Fig. 2. Blood ammonia levels and coma onset in the HE model. Rats first received SST and then underwent partial hepatectomy and/or portal vein stenosis. Animals were then monitored for the onset of coma. Ammonia concentration was measured in blood collected from the abdominal aorta and the mesenteric, portal and postcaval veins 24 h after the surgery or at the onset of coma. A. Blood ammonia levels in various blood vessels in rats. Data represent the mean ± S.D. (n=7–8).* P < 0.05, ** P < 0.01,*** P < 0.001 compared with the SST group. B. Kaplan-Meier curves of coma onset time in 3 independent experiments (n=6-17/experiment).

circulation pathway was changed by a combination of SST and portal vein stenosis, the levels of many serum proteins (aspartate aminotransferase, alanine aminotransferase, creatine kinase, alkaline phosphatase, total bilirubin, total protein, albumin and creatinine) were comparable to those in normal animals (data not shown). However, animals with SST followed by both partial hepatectomy and portal vein stenosis had significantly elevated blood ammonia concentrations in all sampled sites (Fig. 2A). These animals also became comatose. The incidence of coma after HE-inducing surgery increased over time (Fig. 2B), reaching 88% or more in 3 independent experiments (mean =97%).

### 3.3. Effect of rifaximin in the HE model

To clarify the pathological role of GI-derived ammonia in the development of coma in HE, rats were treated with rifaximin, an
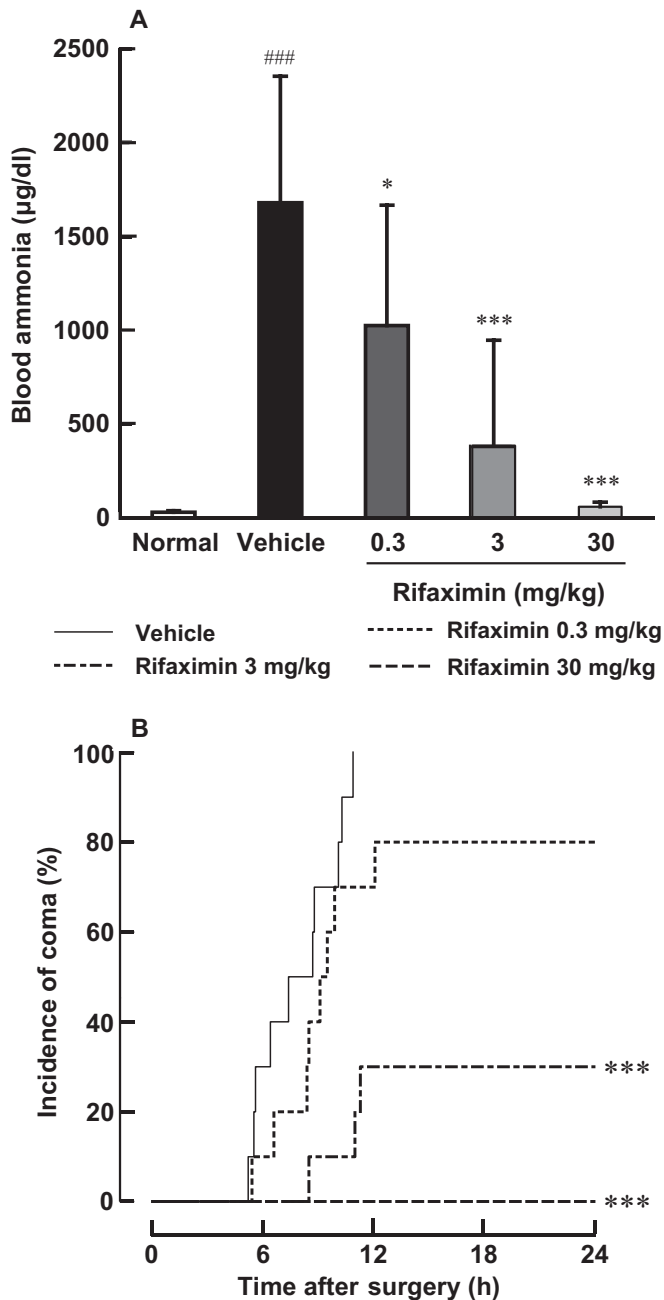
**Fig. 3.** Effects of rifaximin on the incidence of coma and hyperammonemia in the HE model. Rats with SST underwent partial hepatectomy and portal vein stenosis to induce encephalopathy. The onset time of coma was monitored up to 24 h after surgery. Ammonia concentration was measured in blood collected from the postcaval vein at the onset of coma or at 24 h after surgery if no signs of coma were observed. Rifaximin or vehicle was administered orally beginning 3 days before surgery. Normal rats were orally administered vehicle during the same period. A. Effects of rifaximin on blood ammonia levels in HE rats. Data represent the mean ± S.D. (n=10). ### P < 0.001 compared with the normal group and * P < 0.05,*** P < 0.001 compared with the vehicle group. B. Kaplan-Meier curves of coma onset time in HE rats.*** P < 0.001 compared with the vehicle group (n=10).

oral antibiotic that is poorly absorbed. Rifaximin decreases gut flora, thereby decreasing ammonia in the GI tract. In the vehicle group (0.5% Tween 80), the postcaval ammonia concentration increased 50-fold or more compared with the normal group (Fig. 3A). Animals treated with rifaximin showed a dose-dependent inhibition of postcaval ammonia concentrations compared with the vehicle group. In the vehicle group, coma occurred in all 10 animals within 11 h of HE-inducing surgery (Fig. 3B). In

contrast, rifaximin treatment had a dose-dependent effect on coma onset. In the rifaximin groups, coma appeared in 8 of 10 animals (0.3 mg/kg), 3 of 10 animals (3 mg/kg) and 0 of 10 animals (30 mg/kg) within 24 h of HE-inducing surgery. Higher doses of rifaximin (3 and 30 mg/kg) significantly inhibited the onset of coma compared with the vehicle group.

### 3.4. Behavioral changes in the HE model

Encephalopathy was determined by evaluation of pain response, pinna reflex, corneal reflex and passivity over time (Fig. 4). Prior to coma onset, decreased pain responses and increased passivity were noted early after HE-inducing surgery in the vehicle group. Subsequently, pinna and corneal reflexes decreased followed by loss of the righting reflex, indicating the comatose state. Rifaximin treatment (0.3–30 mg/kg) reduced all behavioral changes in a dose-dependent manner. Similar results were obtained in other behavioral evaluations, such as alertness and locomotor activity (data not shown).

### 3.5. Time course of ammonia levels in the HE model

To better understand to pathological progression of HE, ammonia levels in the blood and CSF were measured over time. In addition, serum levels of S100B were measured as a biomarker indicating brain damage or dysfunction. In the vehicle group, the blood ammonia concentration in the splenic vein increased immediately after HE-inducing surgery, reaching a level equivalent to that in the mesenteric vein (Fig. 5A, D). The blood ammonia concentration in the postcaval vein increased gradually, reaching 1000 μg/dl or higher 3 h after surgery. The increased ammonia level in the postcaval vein indicates that portal blood containing high concentrations of ammonia flowed into the peripheral blood through the splenic vein and the collateral vessels. The ammonia concentration in the CSF significantly increased at the onset of coma (Fig. 5B, E). The levels of S100B in the postcaval vein increased with increasing ammonia levels in the CSF during coma (Fig. 5C, F). Rifaximin treatment led to a decrease in ammonia levels in blood and CSF and a decrease in S100B levels in blood.

### 3.6. Histological examination of the brain

We next evaluated brain injury in the HE model by histopathological examination of brain tissues (Fig. 6). In the vehicle group, vacuolar degeneration of astrocytes and perivascular vacuolation in the cerebrum were observed in some animals at 1 h after surgery and in all animals at 3 h after surgery and at the onset of coma. Larger areas of damage were observed at the onset of coma, including vacuolar degeneration of neurons and perineuronal vacuolation (Fig. 6C and D). In animals treated with rifaximin 30 mg/kg, very few histopathological changes were observed in the cerebrum.

### 3.7. ICP and brain weight measurement

We next investigated changes in ICP and brain edema in the HE model. The ICP of normal rats under isoflurane anesthesia decreased slightly over a 12 h period. In the vehicle group, ICP markedly increased 12 h after HE-inducing surgery. This increase was suppressed in a dose-dependent manner in animals treated with rifaximin (Fig. 7A). We then turned our attention to brain edema. The brain was removed at the onset of coma or at 24 h after surgery to determine water content. In the vehicle group, the water content of the brain profoundly increased after surgery. The increase in brain water content was suppressed in a dose-dependent manner in animals treated with rifaximin (Fig. 7B).
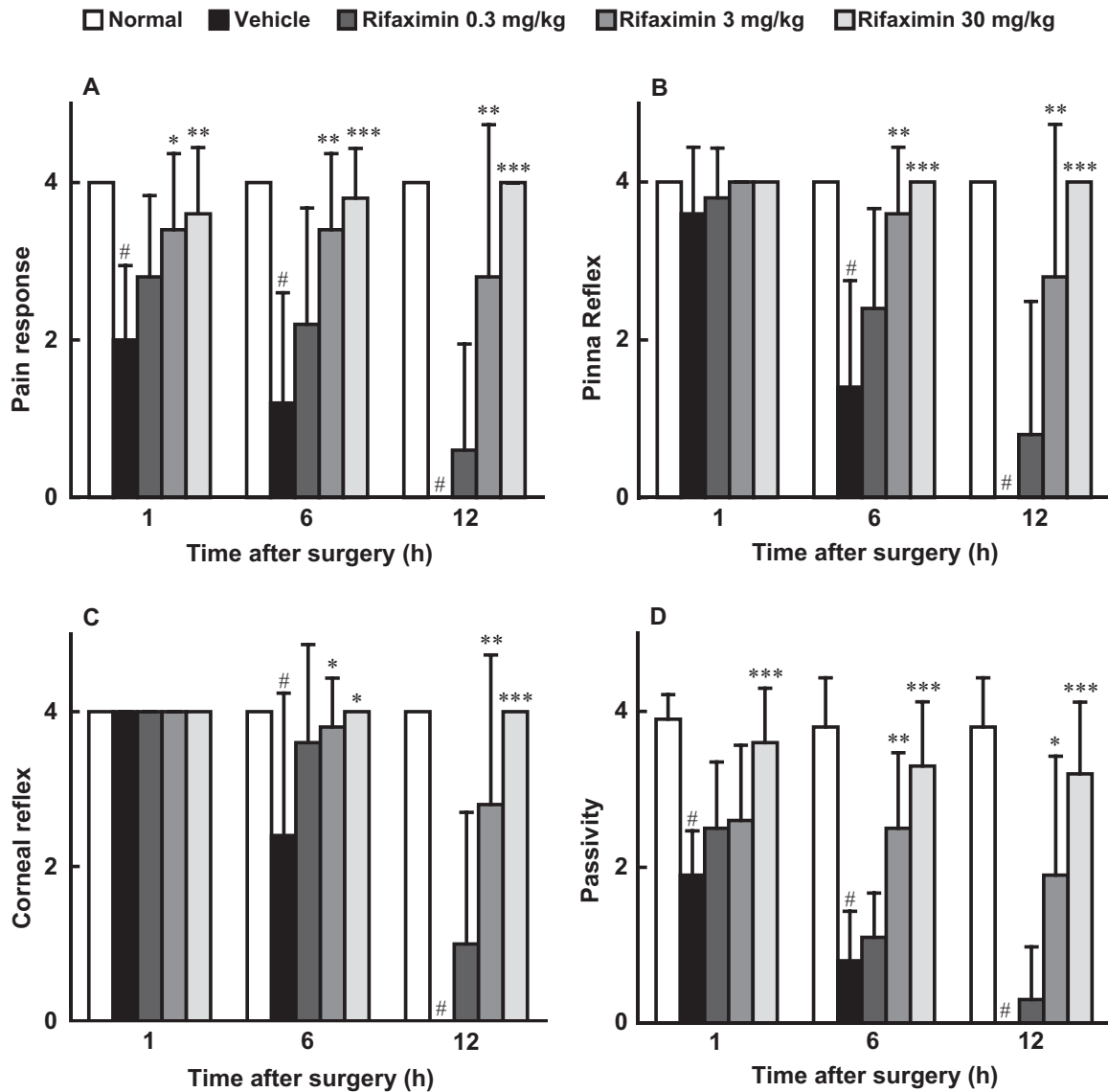
**Fig. 4.** Behavioral disorders in the HE model and effects of rifaximin. Animal behavior was monitored after HE surgery. Rifaximin or vehicle was administered orally beginning 3 days prior to surgery. Normal rats were orally administered vehicle during the same period. Pain response (A), Pinna reflex (B), Corneal reflex (C) and Passivity (D). Data represent the mean $\pm$ S.D. (n=10). # $P < 0.001$ compared with the normal group and * $P < 0.05$,** $P < 0.01$,*** $P < 0.001$ compared with the vehicle group.

### 3.8. Correlation between coma and blood ammonia concentration

In the HE model, the correlation between the time to coma onset and the ammonia concentration in the postcaval vein during coma was investigated. Data from 3 independent experiments were combined. A significant correlation between the time to coma onset and ammonia concentration was observed, with a correlation coefficient of 0.6445 ($P < 0.0001$, Fig. 8).

### 4. Discussion

In order to better understand the pathophysiology of HE in humans, we designed a new animal model of HE. We began our investigations by examining ammonia levels in various blood vessels, as this would provide insight into the origin of hyperammonemia in HE. In normal rats, blood ammonia levels were comparable to those commonly observed in humans (Dam et al., 2011; Ong et al., 2003). We found that the ammonia concentration in portal blood was higher than that in venous blood, confirming

previous findings that ammonia derived from the GI tract is ultimately drained into the portal blood. We further found that the ammonia concentration in mesenteric venous blood, which flows directly from the GI tract to the portal vein, was significantly higher (twice or more) than in portal blood. This fact strongly suggests that the major source of blood ammonia is the GI tract (Nencki et al., 1896; Romero-Gómez, 2005). In the HE model, the ammonia concentration in mesenteric venous blood was more than 10-fold higher than that in venous blood, and was higher than venous concentrations observed in HE patients (Kramer et al., 2000; Ong et al., 2003). These findings indicate that ammonia derived from the GI tract may be a major cause of HE-associated pathology. The primary source of ammonia in the GI tract is enteric bacteria, suggesting that interfering with gut flora, for example with rifaximin, may decrease GI-derived ammonia and thus decrease blood ammonia levels and HE-associated pathology.

To generate our experimental HE model, we first transposed the spleen to the subcutis to achieve a portal venous shunt. After a 4-week recovery period, we confirmed the presence of new collateral vessels around the spleen and verified blood flow between
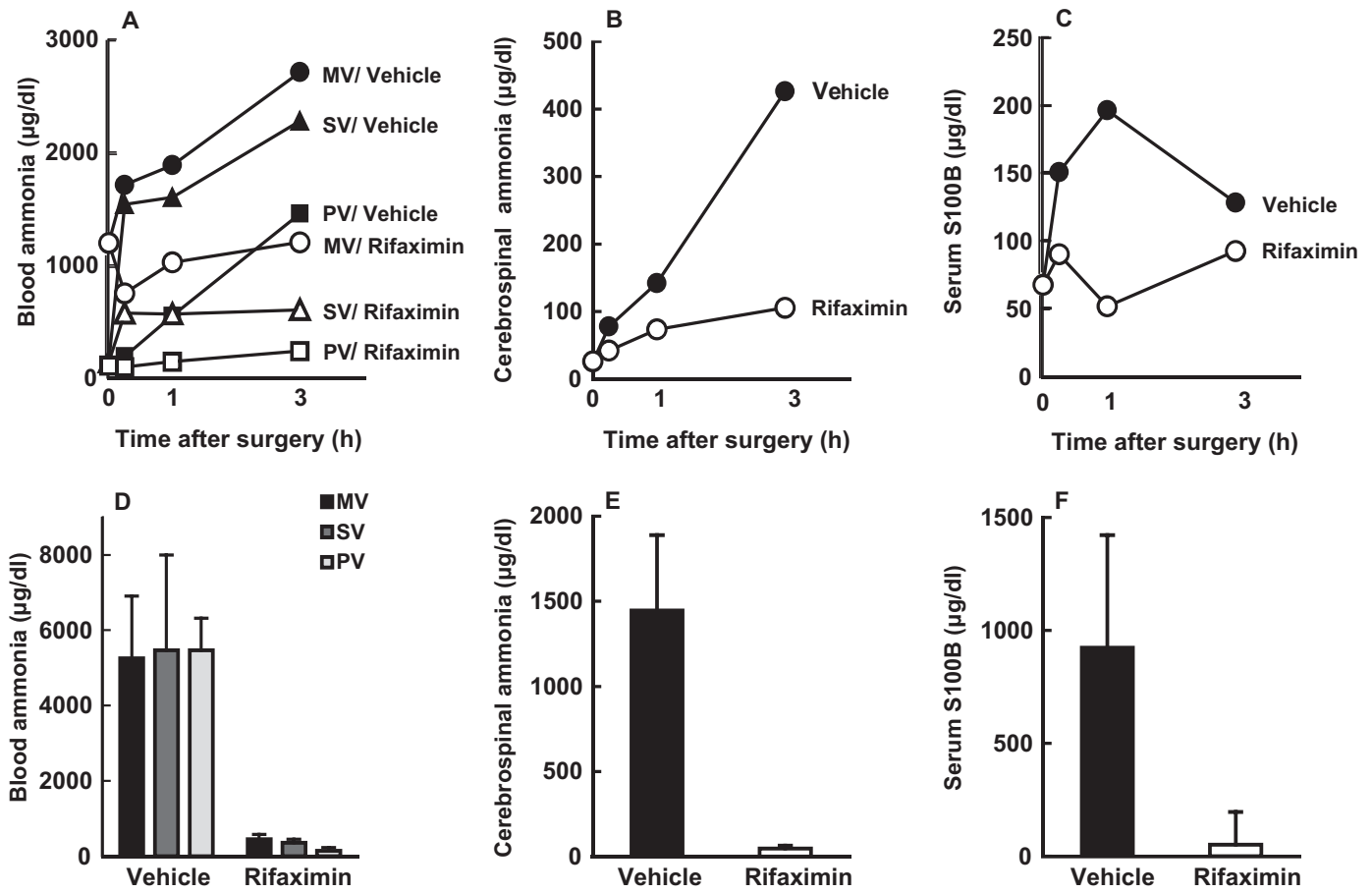
**Fig. 5.** Ammonia levels in the blood and cerebrospinal fluid, S100B levels in the postcaval vein, and effects of rifaximin. Rifaximin (30 mg/kg) or vehicle was administered orally beginning 3 days prior to surgery. Blood in the mesenteric vein (MV), splenic vein (SV) and postcaval vein (PV) as well as cerebrospinal fluid was collected 0, 0.25, 1 and 3 h after HE surgery and at the end of the study. Ammonia levels in the blood and cerebrospinal fluid and serum S100B levels in the PV were determined. The endpoint was 24 h after surgery for rats treated with rifaximin and the onset of coma for rats treated with vehicle. Each graph shows the time course (A–C) and the endpoint (D–F) after HE surgery. Data represent the mean ± S.D. (n=4–9).

these new vessels and the peripheral circulation. We then surgically narrowed the portal vein, re-routing portal blood flow back into the splenic vein and then into the peripheral circulation through the new collateral vessels. This blood flow pattern corresponds to other experimental methods that use bypass graft surgery to achieve a portal-systemic shunt. After SST and portal vein stenosis, hepatic function and serum chemistry values were normal, and animal behaviors were comparable to normal rats. Finally, we partially resected the liver to limit ammonia metabolism. The combination of SST, portal vein stenosis, and partial hepatectomy markedly increased ammonia concentration in the venous blood and led to behavioral changes, including coma. These changes mirrored behavioral changes observed in patients with HE. In contrast to the non-coma inducing experimental models in which liver fibrosis is induced with a choline-deficient diet or with substances containing carbon tetrachloride or thioacetamide (Bengtsson et al., 1987; Méndez et al., 2009; Molinengo et al., 1997), our model has the advantage of allowing analysis of encephalopathy progression. Furthermore, our method uses a simple surgical technique that efficiently alters blood circulation without the need for special bypass graft surgery (portacaval shunting). Animals that underwent HE-inducing surgery exhibited decreased pain response, increased passivity, decreased pinna and corneal reflexes, and finally became comatose. These behavioral changes are similar to those observed prior to coma in patients with chronic liver disease (Vilstrup et al., 2014). Blood ammonia concentration was highest in the mesenteric vein, followed by the

splenic and postcaval veins. Interestingly, the blood ammonia concentration in the postcaval vein exceeded 1000 µg/dl and the concentration in the CSF markedly increased 3 h after surgery. In addition, increased serum levels of S100B, a known index of brain damage (Rothermundt et al., 2003; Wiltfang et al., 1999), in the postcaval vein correlated with increased ammonia concentration in the CSF. We thus investigated histopathological evidence of brain damage in our model. We observed cerebral lesions consisting of vacuolar degeneration of astrocytes. Vacuolation was observed in the perinuclear region of astrocytes and in the perivascular astrocyte foot processes. Moreover, neuronal vacuolar degeneration was observed. These changes are similar to those observed in other HE models, in which astrocyte swelling, Alzheimer type II astrocytes, and perivascular vacuolization have been reported (Jayakumar et al., 2011; Matkowskyj et al., 1999; Pilbeam et al., 1983). It has previously been suggested that the primary pathogenesis of astrocyte swelling is an increase in blood ammonia concentration which triggers oxidative stress, enhanced mitochondrial permeability transition and activation of signaling kinases (Jayakumar et al., 2011; Norenberg et al., 2007). Together, these findings suggest that cerebral damage and related behavioral changes in our HE model are attributable to astrocyte abnormalities caused by increased blood ammonia concentration.

In addition to increased ammonia concentration in the venous blood and coma, increased ICP and brain edema have been reported in patients with ALF (Murphy et al., 2004; Chan et al., 2009; Scott et al., 2013). We thus sought to determine if similar changes
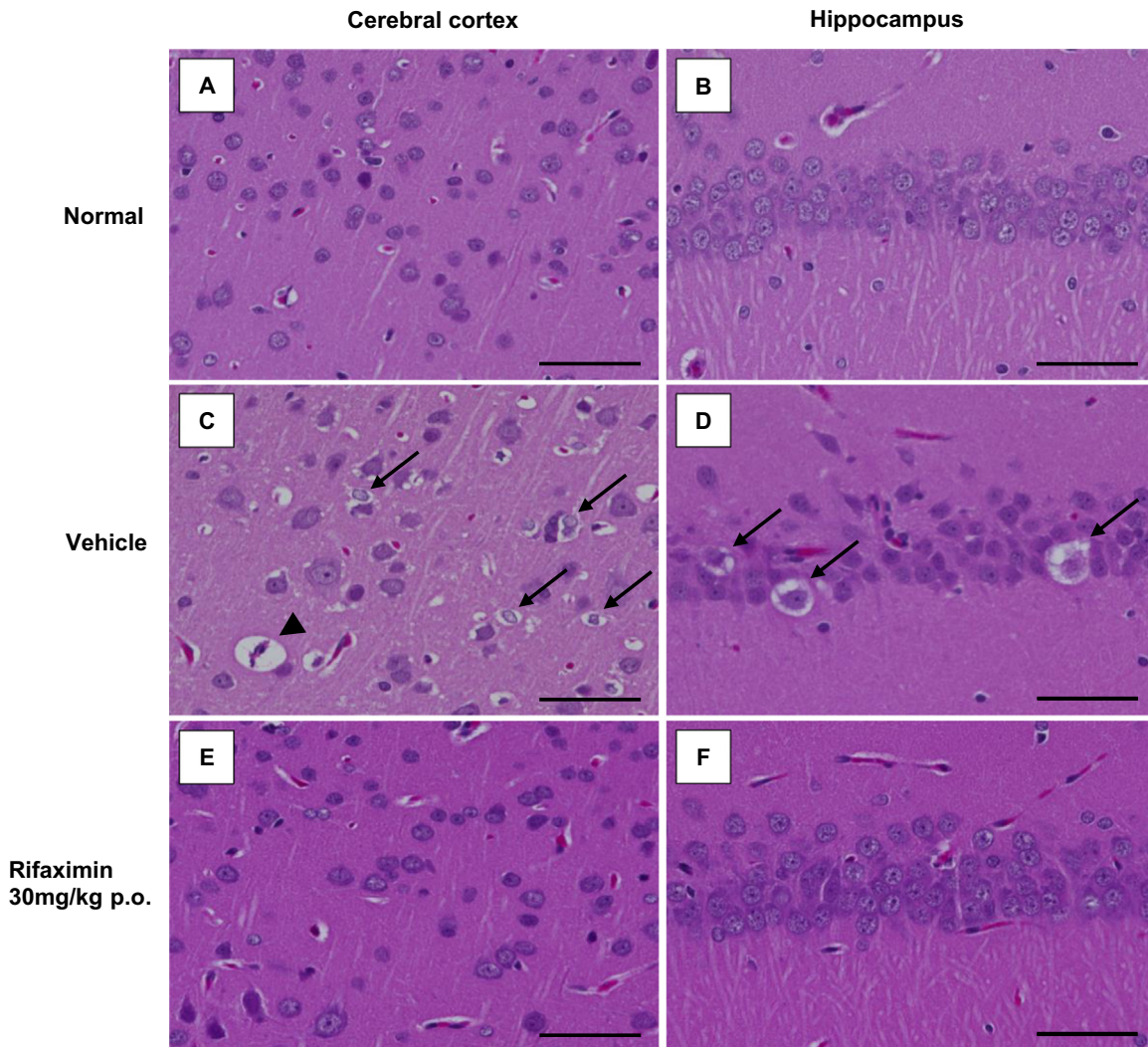
**Cerebral cortex**          **Hippocampus**



**Fig. 6.** Representative photomicrographs of the cerebral cortex (left) and hippocampus (right) in the HE model. Normal morphology was observed in the cerebrum in the normal group (A, B). In HE animals treated with vehicle, vacuolar degeneration of astrocytes or neurons (arrows) was observed in the cerebral cortex (C) or hippocampus (D) and perivascular vacuolation (arrow-head) was observed in the cerebral cortex (C) at the onset of coma. In HE animals treated with rifaximin 30 mg/kg (E, F), no histopathological changes were observed in the cerebrum. Bar $=50\ \mu m$.

occurred in our animal model of HE. We found that both elevated ICP and brain edema were present in animals that developed coma and correlated with elevated CSF ammonia concentrations. Our findings suggest that elevated ammonia levels play an important role in encephalopathy. Blood ammonia levels have recently been shown to correlate with HE severity (Kramer et al., 2000; Ong et al., 2003). Interestingly, we found that acute coma occurred when postcaval blood ammonia concentration exceeded 500 μg/ dl. Additionally, we found a correlation between ammonia concentration in the venous blood and time to coma onset. Hence, our model may be a useful tool with which to investigate the relationship between blood ammonia concentration and HE associated with ALF. The endpoint of this study was the development of coma, and future studies will investigate encephalopathy recovery after releasing stenosis and ameliorating hyperammonemia. The model may also be used to study subacute HE by titrating blood ammonia levels and evaluating subsequent changes in brain function.

Rifaximin is a derivative of rifamycin, which inhibits bacterial DNA-dependent RNA polymerase and has in vitro activities against many aerobic and anaerobic gram-positive and gram-negative bacteria. The bioavailability of rifaximin after oral administration is less than 0.5%. A recent pharmacological study reported that

rifaximin improved hyperammonemia and normalized brain ammonia levels in cirrhotic rats (Òdena et al., 2012). Thus, we evaluated the validity of our HE model using rifaximin. First, we dosed rifaximin to normal rats and confirmed a significant decrease in the ammonia concentration in mesenteric venous blood (data not shown). In the HE model, rifaximin decreased blood ammonia concentrations and decreased the incidence of coma. These results suggest that GI-derived ammonia is an important source of blood ammonia concentration and HE onset. Since rifaximin alters the intestinal flora and reduces bacterial translocation, further research is needed to address these specific effects on HE. On the other hand, glutaminase is known to produce ammonia in the GI tract and high glutaminase activity has been reported in HE patients (Romero-Gómez et al., 2004). It will thus be important to determine the effects of rifaximin on glutaminase activity in our HE model.

In conclusion, we developed a new animal model to investigate the pathologic role of hyperammonemia in HE. HE is a complex pathological state accompanied by personality changes and intellectual disability. Our model reflects both the physiologic and behavioral changes of HE associated with ALF, and recapitulates the clinical benefits of rifaximin treatment. In future studies, the model may be used to further elucidate the pathogenesis of HE associated with hyperammonemia.
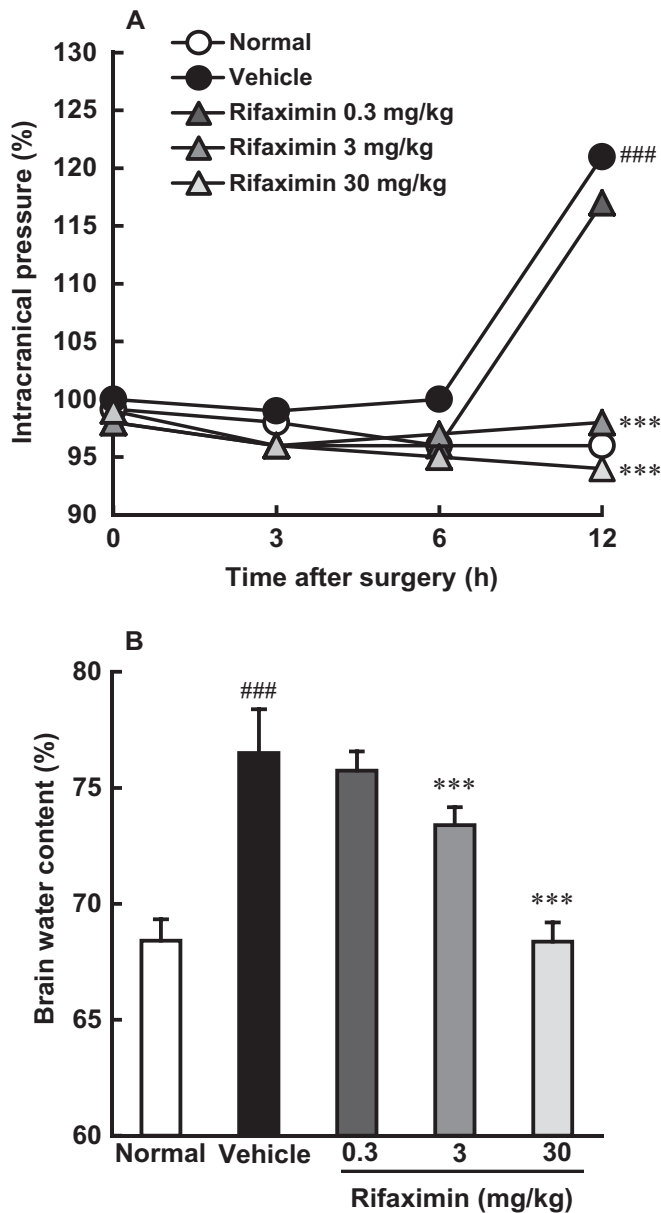
**Fig. 8.** Correlation between the onset time of coma and blood ammonia levels in the HE model. Data obtained from 3 independent experiments are shown as scattergrams (n=4–18/experiment). The correlation coefficient between the onset time of coma and blood ammonia level was 0.6455 (P < 0.0001).



**Fig. 7.** ICP and water content of the brain in the HE model and the effects of rifaximin. A. ICP was measured up to 12 h after HE surgery. Rifaximin or vehicle was administered orally beginning 3 days prior to surgery. Normal rats were orally administered vehicle during the same period. Data represent mean ICP (%, n=6–8). *** P < 0.001 compared with the vehicle group, ### P < 0.001 compared with the normal group. B. Water content was measured in brain tissue collected at the onset of coma or at 24 h after surgery if no signs of coma were observed. Data represent the mean ± S.D. (n=8–9).*** P < 0.001 compared with the vehicle group and ### P < 0.001 compared with the normal group.

# References

Bass, N.M., Mullen, K.D., Sanyal, A., Poordad, F., Neff, G., Leevy, C.B., Sigal, S., Sheikh, M.Y., Beavers, K., Frederick, T., et al., 2010. Rifaximin treatment in hepatic encephalopathy. N. Engl. J. Med. 362, 1071–1081.

Bengtsson, F., Bugge, M., Vagianos, C., Jeppsson, B., Nobin, A., 1987. Brain serotonin metabolism and behavior in rats with carbon tetrachloride-induced liver cirrhosis. Res. Exp. Med. 187, 429–438.

Bernal, W., Hall, C., Karvellas, C.J., Auzinger, G., Sizer, E., Wendon, J., 2007. Arterial ammonia and clinical risk factors for encephalopathy and intracranial hypertention in acute liver failure. Hepatology 46, 1844–1852.

Bosoi, C.R., Parent-Robitaille, C., Anderson, K., Tremblay, M., Rose, C.F., 2011. AST-120 (spherical carbon adsorbent) lowers ammonia levels and attenuates brain edema in bile duct-ligated rats. Hepatology 53, 1995–2002.

Butterworth, R.F., Norenberg, M.D., Felipo, V., Ferenci, P., Albrecht, J., Blei, A.T., 2009. Experimental models of hepatic encephalopathy: ISHEN guidelines. Liver Int. 29, 783–788.
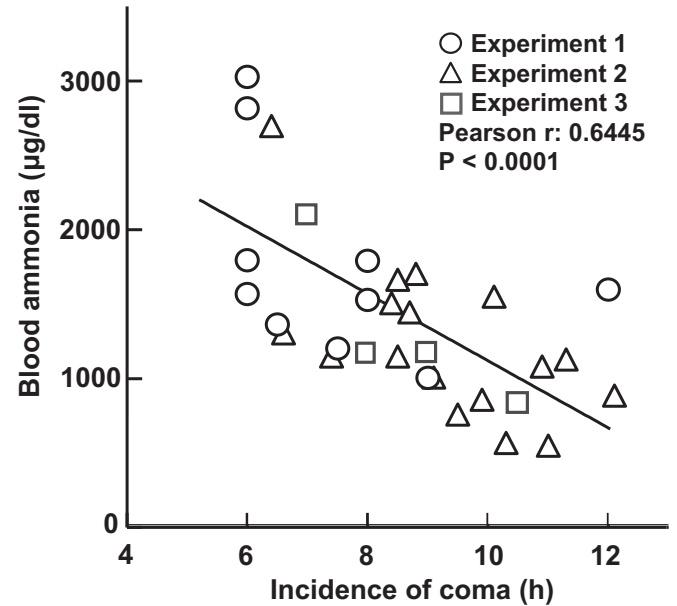
Chan, G., Taqi, A., Marotta, P., Levstik, M., McAlister, V., Wall, W., Quan, D., 2009. Long-term outcomes of emergency liver transplantation for acute liver failure. Liver Transpl. 15, 1696–1702.

Dam, G., Keiding, S., Munk, O.L., Ott, P., Buhl, M., Vilstrup, H., Bak, L.K., Waagepetersen, H.S., Schousboe, A., Møller, N., Sørensen, M., 2011. Branched-chain amino acids increase arterial blood ammonia in spite of enhanced intrinsic muscle ammonia metabolism in patients with cirrhosis and healthy subjects. Am. J. Physiol. Gastrointest. Liver Physiol. 301, G269–G277.

Di Domenico, S., Bovio, G., Gelli, M., Ravazzoni, F., Andorno, E., Cottalasso, D., Valente, U., 2007. Cavo-portal transposition in rat: a new simple model. BMC Surg. . http://dx.doi.org/10.1186/1471-2482-7-18

Ferenci, P., Lockwood, A., Mullen, K., Tarter, R., Weissenborn, K., Blei, A.T., 2002. Hepatic encephalopathy-definition, nomenclature, diagnosis, and quantification: final report of the working party at the 11th World Congresses of Gastroenterology, Vienna, 1998. Hepatology 35, 716–721.

Funovics, J.M., Cummings, M.G., Shuman, L., James, J.H., Fischer, J.E., 1975. An improved nonsuture method for portacaval anastomosis in the rat. Surgery 77, 661–664.

Hahn, M., Massen, O., Nencki, M., Pawlow, J., 1893. Die Eck'sche fistel zwischen der unteren hohlvene und der pfortader und ihre folgen für den organismus. Arch. Exp. Pathol. Pharm. 32, 161–210.

Irwin, S., 1968. Comprehensive Observational Assessment: Ia. a systematic, quantitative procedure for assessing the behavioral and physiologic state of the mouse. Psychophrmacologia 13, 222–257.

Jayakumar, A.R., Bethea, J.R., Tong, X.Y., Gomez, J., Norenberg, M.D., 2011. NF-κB in the mechanism of brain edema in acute liver failure: studies in transgenic mice. Neurobiol. Dis. 41, 498–507.

Jover, R., de Madaria, E., Felipo, V., Rodrigo, R., Candela, A., Compañ, A., 2005. Animal models in the study of episodic hepatic encephalopathy in cirrhosis. Metab. Brain Dis. 20, 399–408.

Kramer, L., Tribl, B., Gendo, A., Zauner, C., Schneider, B., Ferenci, P., Madl, C., 2000. Partial pressure of ammonia versus ammonia in hepatic encephalopathy. Hepatology 31, 30–34.

Leise, M.D., Poterucha, J.J., Kamath, P.S., Kim, W.R., 2014. Management of hepatic encephalopathy in the hospital. Mayo Clin. Proc. 89, 241–253.

Matkowskyj, K.A., Marrero, J.A., Carroll, R.E., Danilkovich, A.V., Green, R.M., Benya, R. V., 1999. Azoxymethane-induced fulminant hepatic failure in C57BL/6J mice: characterization of a new animal model. Am. J. Physiol. 277, G455–G462.

Méndez, M., Méndez-López, M., López, L., Aller, M.A., Arias, J., Arias, J.L., 2009. Associative learning deficit in two experimental models of hepatic encephalopathy. Behav. Brain Res. 198, 346–351.

Molinengo, L., Orsetti, M., Ghi, P., 1997. Behavioral and neurochemical effects of a chronic choline-deficient diet in the rat. Behav. Brain Res. 84, 145–150.

Murphy, N., Auzinger, G., Bernal, W., Wendon, J., 2004. The effect of hypertonic sodium chloride on intracranial pressure in patients with acute liver failure. Hepatology 39, 464–470.

Nencki, M., Zaleski, J., 1895. Ueber die bestimmung des ammoniaks in thierischen flüssigkeiten und geweben. Arch. Exp. Pathol. Pharmakol. 36, 385–394.

Nencki, M., Pawlow, J.P., Zaleski, J., 1896. Ueber den ammoniakgehalt des blutes und der organe und die harnstoffbildung bei den säugethieren. Arch. Exp. Pathol.

Pharmakol. 37, 26–51.

Nikfarjam, M., Malcontenti-Wilson, C., Fanartzis, M., Daruwalla, J., Christophi, C., 2004. A model of partial hepatectomy in mice. J. Invest. Surg. 17, 291–294.

Norenberg, M.D., Jayakumar, A.R., Rama Rao, K.V., Panickar, K.S., 2007. New concepts in the mechanism of ammonia-induced astrocyte swelling. Metab. Brain Dis. 22, 219–234.

Òdena, G., Miquel, M., Serafín, A., Galan, A., Morillas, R., Planas, R., Bartolí, R., 2012. Rifaximin, but not growth factor 1, reduces brain edema in cirrhotic rats. World J. Gastroenterol. 18, 2084–2091.

Ong, J.P., Aggarwal, A., Krieger, D., Easley, K.A., Karafa, M.T., Van Lente, F., Arroliga, A. C., Mullen, K.D., 2003. Correlation between ammonia levels and the severity of hepatic encephalopathy. Am. J. Med. 114, 188–193.

Pilbeam, C.M., Anderson, R.M., Bhathal, P.S., 1983. The brain in experimental portal-systemic encephalopathy. J. Pathol. 140, 331–345.

Riordan, S.M., Williams, R., 1997. Treatment of hepatic encephalopathy. N. Engl. J. Med. 337, 473–479.

Romero-Gómez, M., 2005. Role of phosphate-activated glutaminase in the pathogenesis of hepatic encephalopathy. Metab. Brain Dis. 20, 319–325.

Romero-Gómez, M., Montagnese, S., Jalan, R., 2015. Hepatic encephalopathy in patients with acute decompensation of cirrhosis and acute-on-chronic liver failure. J. Hepatol. 62, 437–447.

Romero-Gómez, M., Ramos-Guerrero, R., Grande, L., de Terán, L.C., Corpas, R., Camacho, I., Bautista, J.D., 2004. Intestinal glutaminase activity is increased in liver cirrhosis and correlates with minimal hepatic encephalopathy. J. Hepatol.

41, 49–54.

Rothermundt, M., Peters, M., Prehn, J.H.M., Arolt, V., 2003. S100B in brain damage and neurodegeneration. Microsc. Res. Tech. 60, 614–632.

Scott, T.R., Kronsten, V.T., Hughes, R.D., Shawcross, D.L., 2013. Pathophysiology of cerebral oedema in acute liver failure. World J. Gastroenterol. 19, 9240–9255.

Shawcross, D.L., Sharifi, Y., Canavan, J.B., Yeoman, A.D., Abeles, R.D., Taylor, N.J., Auzinger, G., Bernal, W., Wendon, J.A., 2011. Infection and systemic inflammation, not ammonia, are associated with grade 3/4 hepatic encephalopathy, but not mortality in cirrhosis. J. Hepatol. 54, 640–649.

Sturgeon, J.P., Shawcross, D.L., 2014. Recent insights into the pathogenesis of hepatic encephalopathy and treatments. Expert Rev. Gastroenterol. Hepatol. 8, 83–100.

Vilstrup, H., Amodio, P., Bajaj, J., Cordoba, J., Ferenci, P., Mullen, K.D., Weissenborn, K., Wong, P., 2014. Hepatic encephalopathy in chronic liver disease: 2014 practice guideline by the European association for the study of the liver and the American association for the study of liver diseases. J. Hepatol. 61, 642–659.

Wiltfang, J., Nolte, W., Otto, M., Wildberg, J., Bahn, E., Figulla, H.R., Pralle, L., Hartmann, H., Rürher, E., Ramadori, G., 1999. Elevated serum levels of astroglial S100β in patients with liver cirrhosis indicate early and subclinical portal-systemic encephalopathy. Metab. Brain Dis. 14, 239–251.

Yamaguchi, F., Etoh, T., Takahashi, M., Misaki, H., Sakuraba, H., Ohshima, T., 2005. A new enzymatic cycling method for ammonia assay using NAD synthetase. Clin. Chim. Acta 352, 165–173.